Electrodynamic constraints on minimum SAR in parallel excitation

R. Lattanzi[1,2], A. K. Grant[2], D. K. Sodickson[1,2], and Y. Zhu[3]

[1]Harvard-MIT Division of Health Sciences and Technology, Cambridge, MA, United States, [2]Radiology, Beth Israel Deaconess Medical Center, Boston, MA, United States, [3]GE Global Research, Niskayuna, NY, United States

Introduction

By making use of multiple independently driven transmit coils, parallel transmission enables acceleration of multidimensional excitation pulses, widening the range of clinical applications for which they can be employed [1,2]. Transmission of tailored radiofrequency (RF) waveforms with the individual elements of a transmit coil array was also shown to provide better management of RF power deposition [2], which is critical for MR imaging at high magnetic field strength. As such applications are explored further, it will be important to investigate the intrinsic constraints of the technique. In the case of parallel imaging, it has been shown that there is an inherent electrodynamic limitation to the achievable SNR for any physically realizable coil array and the behavior of ultimate intrinsic SNR has been extensively studied [3,4]. In this work, we introduce the concept of ultimate intrinsic SAR and we perform a similar investigation for the case of parallel excitation. An inherent lower bound on the power deposition associated to a particular excitation profile was determined for a spherical object by doing a constrained optimization of the electromagnetic field used for transmission, without any assumption about the coil array configuration. These fundamental limitations on SAR optimization in parallel transmission were theoretically investigated, and their dependence on main field strength and acceleration factor were explored.

Theory and Methods

The total RF energy dissipated in the subject, averaged over the excitation period, is given by $\xi = 1/P\sum_1^P \int_V \boldsymbol{\sigma}(\mathbf{r})\left|E(\mathbf{r}, p\Delta t)\right|^2 \Delta t d\mathbf{r}$, where σ is the tissue conductivity, Δt the length of each sampling interval and P the total number of samples in the excitation period. As the electric field scales linearly with the applied currents used to generate RF pulses, and the RF pulses are in turn related to $f^{(n)}(\mathbf{r})$, the periodic excitation patterns**,** by a Fourier transform, using Parseval's theorem, ξ can be expressed as a quadratic form in terms of $\mathbf{f}_p$ [5]: $\xi = 1/P\sum_1^P (\mathbf{f}_p^H \Phi \mathbf{f}_p)$. $\boldsymbol{\Phi}$ is a positive definite covariance matrix. In accelerated parallel excitation, the aliased single-coil excitation patterns are linearly combined such that the aliasing lobes cancel out and the central lobe generates the desired profile. This condition represents the constraint for the design of pulses that minimize power deposition in the subject. We also know that the electromagnetic field inside the subject can be expressed as a sum of weighted basis functions that are multipole expansion solutions of source-free Maxwell's equations [4]. Therefore, in order to calculate the ultimate intrinsic SAR, we have to solve a constrained optimization of the weighting factors, minimizing ξ under the design constraint. For this work, a solution was calculated in the case of EPI-trajectory small tip-angle parallel excitations following a method outlined by Zhu [5]. We used the optimal weighting factors to find the excitation patterns $f^{(n)}(\mathbf{r})$ that result in minimum average SAR. This was carried out one set of aliased pixels (x,y) at a time:

$$\mathbf{f}_p = \Phi^{-1}\mathbf{C}_{x,y}^H(\mathbf{C}_{x,y}\Phi^{-1}\mathbf{C}_{x,y}^H)^{-1}\boldsymbol{\mu}_{x,y},$$

where $\boldsymbol{\mu}_{x,y}$ is the target profile for the set of pixels (x,y), $\mathbf{C}_{x,y}$ contains B_{1+} fields of each mode calculated at positions (x,y) and $\boldsymbol{\Phi}$ is computed using the electric vector basis functions. Ultimate intrinsic SAR is a global measure of the theoretical minimum power deposition during the entire excitation and it is proportional to:

$$SAR_{\text{ult-int}} \propto 1/P\sum_1^P \left[\boldsymbol{\mu}_{x,y}^H(\mathbf{C}_{x,y}\Phi^{-1}\mathbf{C}_{x,y}^H)^{-1}\boldsymbol{\mu}_{x,y}\right]_p .$$

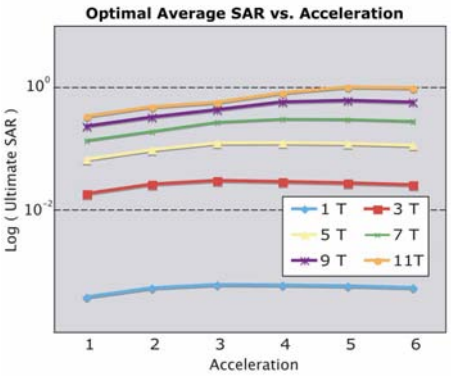

Fig. 1 Ultimate intrinsic SAR in uniform excitation of a 64x64 axial slice for various acceleration factors at different field strengths.

The net electric field associated with each optimal excitation can be calculated by weighting the electric vector basis functions with the Fourier transform of the corresponding elements of $\mathbf{f}_p$. Knowledge of the net electric field during each excitation sampling interval enables calculation of the power deposition at each pixel location as a function of time and thus provides us with spatial SAR distribution while moving through excitation k-space. A uniform target profile throughout a section in the center of a homogeneous sphere with diameter of 0.15 m was employed to calculate ultimate intrinsic SAR and to investigate where and when SAR peaks occur. The algorithm was implemented on a standard PC using MATLAB (Mathworks, Natick, USA). Calculations were performed for different main magnetic field strength values and for various acceleration factors. The electromagnetic properties of the material were chosen as in a previous study [4].

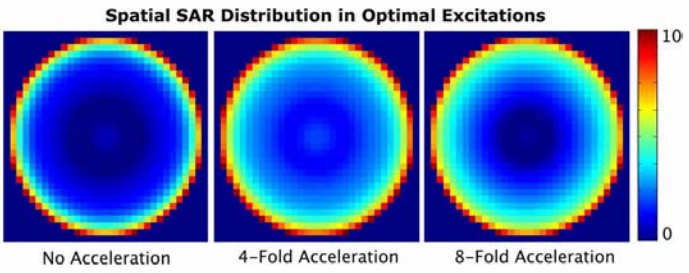

Fig. 2 Normalized SAR distribution (log scale) within the FOV during excitation with optimal current patterns of the center of k-space at 7T field strength for fully sampled, 4-fold accelerated and 8-fold accelerated cases.

Results and Discussion

Figure 1 shows calculated ultimate SAR behavior as a function of the acceleration factor for various field strengths. As expected the average minimum power deposition to the subject increases as we move to higher B_o. However, the increment in SAR decreases with increasing field strength, suggesting that the higher the field strength is, the more effective parallel excitation becomes in minimizing SAR. It is also seen that as the acceleration factor (R) increases, ultimate SAR grows up to a critical acceleration factor R_{crit} and beyond that begins to fall. There is an evident dependency on B_o, as R_{crit} increases by one unit for every 4 Tesla increase of the main magnetic field. Spatial SAR distribution also changes with acceleration factor, as demonstrated in Figure 2 for 7T field strength. For 4-fold acceleration, ultimate SAR is higher everywhere than for the unaccelerated case, whereas for 8-fold acceleration, ultimate SAR in the center of the object falls below that of the unaccelerated case. These observations are in accordance with current arguments that average SAR may not be the only important parameter in assessing MR safety and that attention should also be paid to local SAR values.

Conclusions

We have described a procedure for calculating ultimate SAR for a given k-space excitation scheme. The calculations reported here reveal a fundamental and somewhat unexpected B_o-dependent relation between the optimal SAR and the acceleration factor. Future work is necessary to formalize this relation. Periodic excitation patterns resulting in optimal SAR were calculated and used to map spatial SAR distribution as a function of time. In general, it was found that power deposition localizes near the edge of the object, but that the degree of localization changes as acceleration increases.

References

[1] Katscher U et al, (2003) MRM 49: 144-150;
[2] Zhu Y, (2004) MRM 51: 775-784;
[3] Ohliger MA et al, (2003) MRM 50: 1018-1030;
[4] Wiesinger F et al (2004) MRM 52: 953-964;
[5] Zhu Y, ISMRM 2006, 599.